Journal of Innovative Materials in Extreme Conditions
2023
Volume 4
Issue 1

DFT STUDY OF CRYSTALLINE TiO_2 PHASE TRANSITIONS APPLICABLE IN EXTREME ENVIRONMENTS

Dušica Jovanović[1,2]*, Dejan Zagorac[1,3], Aleksandra Zarubica[2], Matej Fonović[4], Jelena Zagorac[1,3]

[1]*Institute of Nuclear Sciences Vinča, Materials Science Laboratory, University of Belgrade, Belgrade, Serbia*
[2]*Department of Chemistry, Faculty of Science and Mathematics, University of Niš, Niš, Serbia*
[3] *Center for Synthesis, Processing, and Characterization of Materials for Application in the Extreme Conditions-CextremeLab, Belgrade, Serbia*
[4]*Faculty of Engineering, University of Rijeka-RiTeh, Rijeka, Croatia*
Corresponding author: dusica.jovanovic011@gmail.com*

Abstract: *Crystalline TiO_2 has many practical applications as a photocatalytic material. The structures and relative energies of eleven different modifications of bulk structures with TiO_2 composition were theoretically investigated in this study. Calculations were performed by the DFT method with LDA-PZ functional as implemented in CRYSTAL17 code. Structural parameters, energy-volume curves and electronic band gaps were calculated and analyzed. This study aimed to gain insight into the electronic structure of various modifications of crystalline pristine TiO_2 and their phase transitions especially applicable at extreme pressure and temperature conditions. The information obtained in this study may contribute to future research on the structure and various properties (electronic, mechanical…) of such systems, as well as their potential application in various scientific fields and advanced technology.*

Keywords**:** *crystalline TiO_2, phase transitions, EV curves, DFT, ab initio*

1. Introduction

Titanium dioxide (TiO_2) is a widely investigated transition metal oxide, both experimentally and theoretically [1]. TiO_2 is attracting attention as a wide band gap semiconductor with photocatalytic properties and applicability in various fields (production of solar cells, decontamination of pollutants, elimination of microorganisms, suppression of cancer cells, etc.)[1-5]. Experimental and theoretical studies of this material can provide different data on the stability of certain crystal modifications and their transitions. In addition to the most known crystalline TiO_2 structures, anatase ($I4_1/amdz$) and rutile ($P4_2/mnm$), some modifications can be found in nature, theoretically simulated and obtained experimentally under certain conditions with the following space groups: *Pbca* (brookite), *C*2/*m* (TiO_2-B), $P2_1/c$ (ZrO_2), $P3_12_1$ (quartz-low), *Pa*-3 (pyrite), *Fm*-3*m* (fluorite), *Pbcn* (TiO_2-II), *P*-62*m* (Fe_2P type), *Pbnm* (TiO_2-R) [6-8], which structural parameters obtained experimentally or theoretically can be found in ICSD (Inorganic Crystal Structure Database) [9, 10]. The most thermodynamically stable TiO_2 modification is tetragonal rutile, but at elevated temperatures, metastable tetragonal anatase and metastable orthorhombic brookite irreversibly transform to rutile[1]. By investigating a wide range of TiO_2 modifications and their phase transitions, one can gain insight into their structure-property relation and the necessary conditions for future potential experimental/theoretical research [11-13]. The important information on their optical and electronic properties is a direct band gap energy value determined for rutile 3.02 eV and for anatase 3.2 eV [6-8, 14] which narrowing can be enabled by doping with different cations and anions [15-17]. In this theoretical study, we will present the structural parameters, band gap values, and energy-volume curves for different modifications of crystalline TiO_2.

2. Computational details

We have completed *ab initio* calculations using the CRYSTAL17 [18, 19] software package, which is based on the linear combination of atomic orbitals (LCAO) as the basis set. We have used all-electron basis sets (AEBS) for calculations – a [4s3p1d] for titanium [20, 21] and [4s3p] for oxygen [17, 22, 23]. Local optimizations have been performed by the density functional theory (DFT) method with exchange-correlation functional, local density approximation (LDA) with the Perdew–Zunger (PZ) correlation functional[24]. A search for structure candidates that might exist in extreme conditions has been conducted adopting experimental data as initial structures for calculations from the Inorganic Crystal Structure Database (ICSD) [9, 10]. It is of great importance to analyze the effect of extreme conditions on structural and electronic properties, as well as on the structure-property relationship.[25-28] All obtained results have been analyzed in the KPLOT software package [29] and visualized by the VESTA program [30].

3. Results and discussion

3.1. Structural properties of various bulk TiO_2 modifications

For TiO_2 composition, we have performed a data mining-based search of the Inorganic Crystal Structure Database (ICSD). In this way, we have found 11 different structure candidates for local optimization. Most of the candidates already exist for the TiO_2 composition (anatase, rutile, *Pbca* (brookite), *C*2/*m* (TiO_2-B), $P2_1/c$ (ZrO_2), $P3_12_1$ (quartz-low), *Pbcn* (TiO_2-II), *P*-62*m* (Fe_2P), *Pbnm* (TiO_2-R). Additionally, we have considered two more structure candidates with the general formula AB_2 that have been found in some common minerals: *Pa*-3 (pyrite), and *Fm*-3*m* (fluorite).

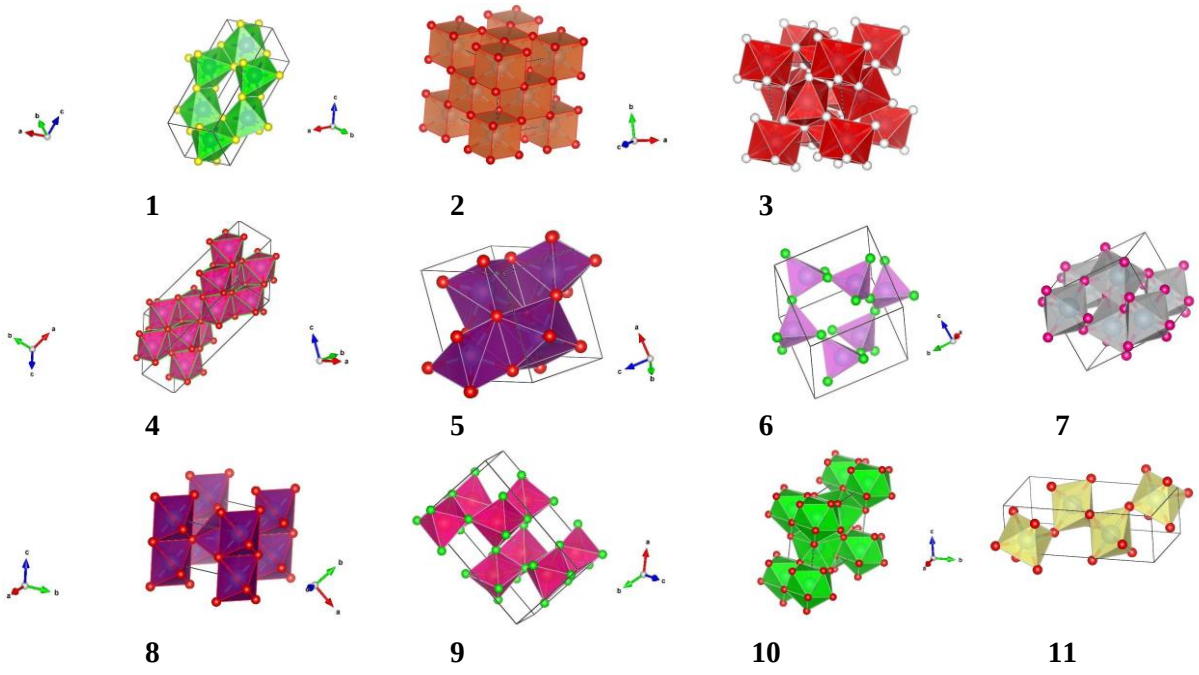

Figure 1. Structures of eleven different TiO_2 modifications: **1**) anatase, **2**) fluorite, **3**) pyrite, **4**) TiO_2-B, **5**) ZrO_2, **6**) quartz-low, **7**) TiO_2-II, **8**) rutile, **9**) brookite, **10**) Fe_2P, **11**) TiO_2-R, adopted from the ICSD database and visualized by VESTA program.

Figure 1 shows 11 different structure types that were considered as the starting modifications for TiO_2 composition during local *ab initio* optimization. Structures have been visualized in the

VESTA program.[30] For each structure shown above the coordination polyhedra around titanium cation and the connection between them differs.

Optimized structure parameters for 11 different starting structure types in TiO_2 and presented in Table 1. Furthermore, total energies per formula unit and detailed crystallographic analysis of the calculated structures using LDA-PZ functional and comparison to the experimental data from the ICSD database [9, 10] have been performed and presented in Table 1. Structures are ranked according to the total energy values in Hartrees (Ha). For each investigated modification, the band gap value has been also calculated and presented in Table 1.

Table 1. Experimental and calculated unit cell parameters, total energies per formula unit, and band gap energies of TiO_2 bulk crystalline modifications investigated by the DFT method and LDA-PZ functional, using CRYSTAL17 code

	Modification	Space group, unit cell parameters (Å) and atomic coordinates		Energy/ formula unit (Ha)	Band gap energy (eV)
		Experimental data	Calculated data		
1.	**TiO_2-II (Columbite)**	*Pbcn* (SG 60) a = 4.53, b = 5.50 c = 4.90 **Ti1** 0 0.1704 0.25 **O1** 0.2716 0.3814 0.4142	*Pbcn* (SG 60) a = 4.50, b = 5.41 c = 4.87 **Ti1** 0 0.6724 0.75 **O1** 0.2746 0.8820 0.9175	−997.1031	2.8
2.	**Rutile**	$P4_2/mnm$ (SG 136) a = 4.65, c = 2.96 **Ti1** 0 0 0 **O1** 0.305 0.305 0	$P4_2/mnm$ (SG 136)[a] a = 4.52, c = 2.94 **Ti1** 0 0 0 **O1** 0.6965 0.6965 0	−997.1018	1.9
3.	**ZrO_2**	$P2_1/c$ (SG 14) a = 4.87, b = 4.92 c = 5.11, β = 99.90 **Ti1** 0.276 0.058 0.217 **O1** 0.062 0.321 0.355 **O2** 0.449 0.759 0.459	$P2_1/c$ (SG 14) a = 4.72, b = 4.82, c = 4.95, β = 98.92 **Ti1** 0.276 0.542 0.211 **O1** 0.071 0.836 0.339 **O2** 0.443 0.258 0.476	−997.1008	2.5
4.	**Brookite**	*Pbca* (SG 61) a = 9.28, b = 5.52 ***c*** = 5.18 **Ti1** 0.129 0.092 0.862 **O1** 0.230 0.108 0.536 **O2** 0.010 0.149 0.183	*Pbca* (SG 61) a = 5.37, b = 5.10 c = 9.09 **Ti1** 0.597 0.854 0.629 **O1** 0.609 0.528 0.730 **O2** 0.649 0.182 0.513	−997.1006	2.7
5.	**TiO_2-B**	*C*2/*m* (SG 12) a = 12.19, b = 3.75 c = 6.53, β = 107.04 **Ti1** 0.196 0 0.292 **Ti2** 0.101 0 0.701 **O1** 0.142 0 0.025 **O2** 0.060 0 0.360 **O3** 0.365 0 0.298 **O4** 0.266 0 0.667	*C*2/*m* (SG 12) a = 12.17, b = 3.68 Å c = 6.49, β = 106.85 **Ti1** 0.805 0 0.712 **Ti2** 0.900 0 0.290 **O1** 0.863 0 0.996 **O2** 0.941 0 0.630 **O3** 0.638 0 0.701 **O4** 0.738 0 0.353	−997.0993	3.1
6.	**Anatase**	$I4_1/amdz$ (SG 141) a = 3.78 c = 9.53 **Ti** 0 0.25 0.3750 **O** 0 0.25 0.1678	$I4_1/amdz$ (SG 141)[a] a = 3.71 c = 9.69 **Ti** 0 0.25 0.8750 **O** 0.5 0.75 0.1701	−997.0983	2.7

7.	**TiO_2-R**	*Pbnm* (SG 62) *a* = 4.90, *b* = 9.46 *c* = 2.96 **Ti1** 0.935 0.137 0.25 **O1** 0.637 0.266 0.25 **O2** 0.208 −0.0276 0.25	*Pbnm* (SG 62) *a* = 5.21, *b* = 3.04 *c* = 6.09 **Ti1** 0.744 0.75 0.618 **O1** 0.859 0.75 0.927 **O2** 0.526 0.25 0.841	−997.0882	2.2
8.	**Fe_2P**	*P*-62*m* (SG 189**)** *a* = 5.33, *c* = 3.13 Å **Ti1** 0.3333 0.6667 0.5 **Ti2** 0 0 0 **O1** 0.263 0 0.5 **O2** 0.601 0 0	*P*-62*m* (SG 189**)** *a* = 5.24, *c* = 3.03 **Ti1** 0.333 0.667 0 **Ti2** 0 0 0.5 **O1** 0.261 0 0 **O2** 0.599 0 0.5	−997.0863	1.3
9.	**Pyrite**	*Pa*-3 (SG 205) *a* = 4.90 **Ti** 0 0 0 **O** 0.341 0.341 0.341	*Pa*-3 (SG 205) *a* = 4.81 **Ti** 0 0.5 0 **O** 0.659 0.159 0.341	−997.0839	1.6
10.	**Fluorite**	*Fm*-3*m* (SG 225) *a* = 4.84 **Ti** 0 0 0 **O** 0.25 0.25 0.25	*Fm*-3*m* (SG 225) *a* = 4.74 **Ti** 0 0 0 **O** 0.75 0.75 0.75	−997.0802	1.4
11.	**Quartz-low**	$P3_12_1$ (SG 152) *a* = 5.29, *c* = 6.13 **Ti1** 0.453 0 0.333 **O1** 0.408 0.303 0.215	$P6_422$ **(**SG 181) *a* = 5.70, *c* = 6.28 **Ti1** 0.5 0 0 **O1** 0.438 0.219 0.833	−997.0688	3.7

[a]**Ref. [17]**

Results of local *ab initio* optimization for eleven different TiO_2 crystalline modifications, using LDA-PZ, showed the lowest total energy calculated for the TiO_2-II (SG 60), suggesting it as the most stable modification. Under normal conditions, rutile is the most stable TiO_2 modification and according to the literature, it undergoes a first-order phase transition to a denser orthorhombic phase, TiO_2-II at pressures above 4 GPa and temperature above 400 °C. [31, 32] The TiO_2-II phase is also known as columbite and in previous research, it has been found that LDA functional produces a stability sequence, $E_{columbite} < E_{anatase} < E_{rutile}$.[33], as has been observed in our study. However, the LDA approximation in combination with the LCAO basis set could be a very good tool for the exploration of materials at extreme conditions of pressure and temperature.

It should be noted that the initial symmetry of the two different structure types (anatase and rutile) did not change after DFT structure optimization[17], while modification quartz-low (SG 152) become more symmetrical and appeared in space group $P6_422$ **(**SG 181), characteristic for quartz-high modification. These newly appeared space groups could be subgroups of the same structures, (or caused by the initial layer structure type adopted from the ICSD database).

Considering electronic properties and band gap values given in Table 1, we can see that all structure types exhibit semiconducting properties, where the lowest value for the band gap (1.3 eV) is found in Fe_2P modification and the highest value (3.7 eV) in the quartz-low modification. It can be noticed that the calculated band gap values for anatase (2.7 eV) and rutile (1.9 eV) were lower than the known, experimentally obtained values (3.2 for anatase and 3.02 for rutile), which is to be expected since DFT-LDA usually underestimates the size of the band gap.

3.2. Phase transitions of crystalline TiO_2 modifications

To further study the crystal structures and their relationship with energy versus volume, *E(V)* curves have been computed on the *ab initio* level (Figure 2). When comparing the minima of the total energy for seven selected different structure types in pure TiO_2, the TiO_2-II type appears to be the most stable. This structure type can exist in TiO_2 in a high-pressure regime[34]. The rutile structure type was found second according to total energy ranking. Brookite and anatase are also found in the negative pressure regions according to the *E(V)* diagram.

According to the enthalpy-pressure curves in Figure 3, the transition from the most stable TiO_2-II modification to the ZrO_2 modification appears at the pressure of 4 GPa. With further pressure increment, ZrO_2 modification can transform to TiO_2-R at approximately 23 GPa.

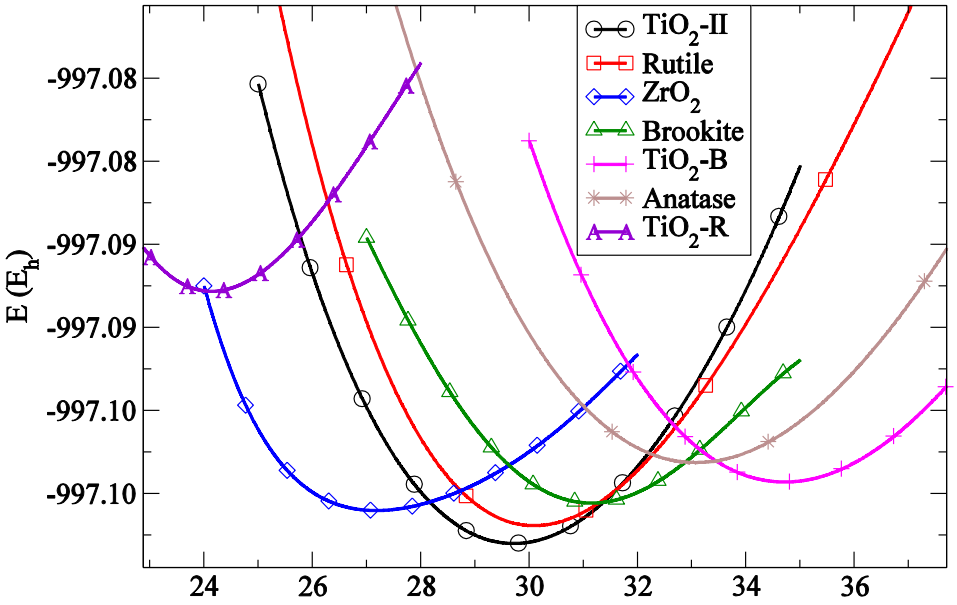

Figure 2. Energy-volume, *E(V)* curves of seven different crystalline TiO_2 modifications computed using LDA-PZ functional.

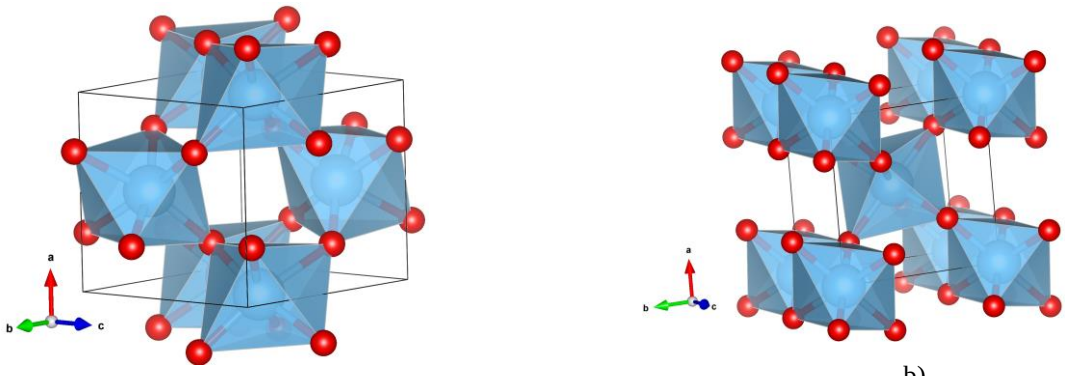

a) b)

Figure 3. Crystal structure of a) TiO_2-II (columbite) and b) rutile structure. Titanium and oxygen atoms are represented by blue and red spheres, respectively.

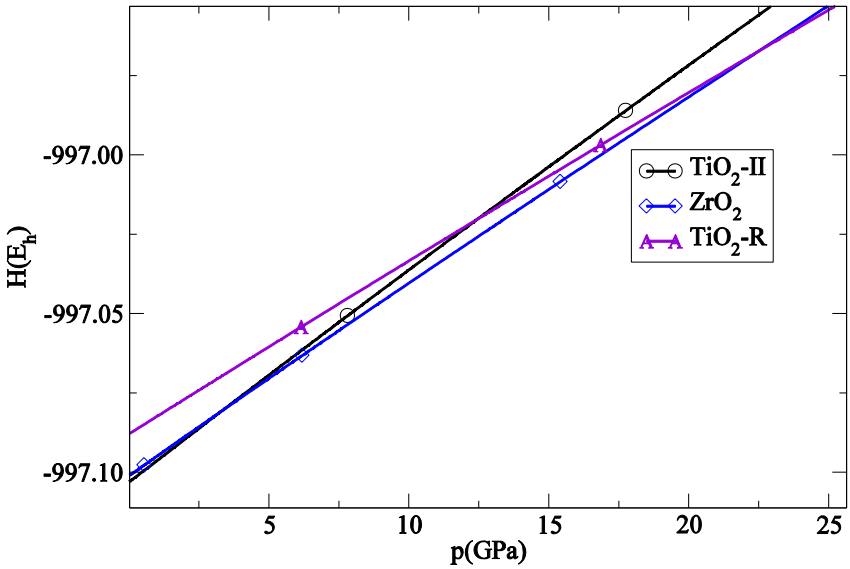

Figure 3. Enthalpy-pressure, *H(p)* curves in the high-pressure region computed using LDA-PZ functional.

4. Conclusion

In this study, we have performed *ab initio* calculations using DFT approximation with an exchange-correlation functional LDA-PZ within the CRYSTAL17 software package. Detailed structural properties after *ab initio* optimization for eleven different crystalline TiO_2 modifications are obtained. According to the *E(V)* curves for seven different modifications and ranking in total energy, the most stable modification is the TiO_2-II. This structure type in a high-pressure regime transforms to ZrO_2 and TiO_2-R modification. We can conclude that *ab initio* results for TiO_2 polymorphs are very sensitive to the choice of the functional and basis sets, and thus, one should be careful when selecting a computational methodology to investigate it. However, chosen LDA-PZ method with the LCAO basis set can be a useful tool for the investigation of structures under extreme conditions.

The band gap values for all investigated modifications have been calculated. The experimental data implicates the rutile structure as the most thermodynamically stable, while previous theoretical data suggest the lowest total energy for the TiO_2-II (columbite) type structure. *E(V)* curves diagram shows very close minimums of TiO_2-II and rutile structures, which is more in agreement with the available literature. After the DFT structure optimization, the quartz-low modification $P3_12_1$ (SG 152) shifted into the higher space group $P6_422$ (SG 181), characteristic of quartz-high modification. The band gap values calculated in this research are lower than those obtained experimentally for anatase and rutile structures, as expected from the LDA functional. The results obtained in this study provide information that should contribute to future research of these systems, as well as to their potential scientific and technological applications, especially in extreme conditions.

Acknowledgments

This work was financially supported by the Ministry of Science, Technological Development and Innovation of the Republic of Serbia through Contract No. 451-03-47/2023-01/200017. The authors are grateful to Prof. R. Dovesi, Prof. K. Doll, and Crystal Solutions for software support with CRYSTAL code. The authors thank the Max Planck Institute for Solid State Research, Stuttgart, Germany, for collaboration and for providing computational support. Furthermore, authors acknowledge the support of the Center of Advanced Computing and Modelling at the University of Rijeka for providing computing resources.

References

[1] M. Vasic, Optimisation and photocatalytic application of nanostructured TiO_2, Department of chemistry of the Faculty of Science and Mathematics, University of Nis, Nis, 2017.
[2] K. Hashimoto, H. Irie, A. Fujishima, TiO_2 Photocatalysis: A Historical Overview and Future Prospects, *Japanese Journal of Applied Physics*, 44 (2005) 8269-8285.
[3] S.M. Gupta, M. Tripathi, A review of TiO_2 nanoparticles, *Chinese Science Bulletin*, 56 (2011) 1639.
[4] M.P. Vinardell, M. Mitjans, Antitumor Activities of Metal Oxide Nanoparticles, *Nanomaterials* (Basel), 5 (2015) 1004-1021.
[5] K. Huang, L. Chen, J. Xiong, L. Meixiang, Preparation and Characterization of Visible-Light-Activated Fe-N Co-Doped TiO_2 and Its Photocatalytic Inactivation Effect on Leukemia Tumors, *International Journal of Photoenergy*, 2012 (2012).
[6] I.J. Ani, U.G. Akpan, M.A. Olutoye, B.H. Hameed, Photocatalytic degradation of pollutants in petroleum refinery wastewater by TiO_2 and ZnO-based photocatalysts: Recent development, *Journal of Cleaner Production*, 205 (2018) 930-954.
[7] B. Babić, A. Zarubica, T.M. Arsić, J. Pantić, B. Jokić, N. Abazović, B. Matović, Iron doped anatase for application in photocatalysis, *Journal of the European Ceramic Society*, 36 (2016) 2991-2996.
[8] A. Krstic, Stankovic, H., Rubezic, M., Vasic, M., Zarubica, A., Chemical modifications of nanostructured titania-based materials in photocatalytic decomposition/conversion of various organic pollutants: A short review, *Advanced Technologies*, 7(2) (2018) 78-84.
[9] G. Bergerhoff, I.D. Brown, Crystallographic Databases, International Union of Crystallography, Chester, UK, 1987.
[10] D. Zagorac, H. Muller, S. Ruehl, J. Zagorac, S. Rehme, Recent developments in the Inorganic Crystal Structure Database: theoretical crystal structure data and related features, *Journal of Applied Crystallography*, 52 (2019) 918-925.
[11] Q.-J. Li, B.-B. Liu, High pressure structural phase transitions of TiO_2 nanomaterials, *Chinese Physics B*, 25 (2016) 076107.
[12] Q.-J. Liu, Z. Ran, F.-S. Liu, Z.-T. Liu, Phase transitions and mechanical stability of TiO_2 polymorphs under high pressure, *Journal of Alloys and Compounds*, 631 (2015) 192-201.
[13] S. Kalaiarasi, A. Sivakumar, S.A. Martin Britto Dhas, M. Jose, Shock wave induced anatase to rutile TiO_2 phase transition using pressure driven shock tube, Materials Letters, 219 (2018) 72-75.
[14] R. Sikora, Ab initio study of phonons in the rutile structure of TiO_2, *Journal of Physics and Chemistry of Solids*, 66 (2005) 1069-1073.
[15] C. Byrne, L. Moran, D. Hermosilla, N. Merayo, Á. Blanco, S. Rhatigan, S. Hinder, P. Ganguly, M. Nolan, S.C. Pillai, Effect of Cu doping on the anatase-to-rutile phase transition in TiO_2 photocatalysts: Theory and experiments, *Applied Catalysis B: Environmental*, 246 (2019) 266-276.
[16] N. Khatun, S. Tiwari, C.P. Vinod, C.-M. Tseng, S.W. Liu, S. Biring, S. Sen, Role of oxygen vacancies and interstitials on structural phase transition, grain growth, and optical properties of Ga doped TiO_2, *Journal of Applied Physics*, 123 (2018) 245702.
[17] D. Jovanović, D. Zagorac, B. Matović, A. Zarubica, J. Zagorac, Anion substitution and influence of sulfur on the crystal structures, phase transitions, and electronic properties of mixed TiO_2/TiS_2 compounds, *Acta Crystallographica Section B*, 77 (2021) 833-847.
[18] R. Dovesi, A. Erba, R. Orlando, C.M. Zicovich-Wilson, B. Civalleri, L. Maschio, M. Rérat, S. Casassa, J. Baima, S. Salustro, B. Kirtman, Quantum-mechanical condensed matter simulations with CRYSTAL, *WIREs Computational Molecular Science*, 8 (2018) e1360.
[19] R. Dovesi, F. Pascale, B. Civalleri, K. Doll, N.M. Harrison, I. Bush, P. D'Arco, Y. Noël, M. Rérat, P. Carbonnière, M. Causà, S. Salustro, V. Lacivita, B. Kirtman, A.M. Ferrari, F.S. Gentile, J. Baima, M. Ferrero, R. Demichelis, M.D.L. Pierre, The CRYSTAL code, 1976–2020 and beyond, a long story, *The Journal of Chemical Physic*s, 152 (2020) 204111.

[20] J. Scaranto, S. Giorgianni, A quantum-mechanical study of CO adsorbed on TiO_2: A comparison of the Lewis acidity of the rutile (110) and the anatase (101) surfaces, *Journal of Molecular Structure: THEOCHEM*, 858 (2008) 72-76.
[21] I. Cvijović-Alagić, Z. Cvijović, D. Zagorac, M.T. Jovanović, Cyclic oxidation of Ti_3Al-based materials, *Ceramics International*, 45 (2019) 9423-9438.
[22] M.D. Towler, N.L. Allan, N.M. Harrison, V.R. Saunders, W.C. Mackrodt, E. Aprà, Ab initio study of MnO and NiO, *Physical Review B*, 50 (1994) 5041-5054.
[23] J. Zagorac, J.C. Schön, B. Matović, T. Škundrić, D. Zagorac, Predicting Feasible Modifications of Ce_2ON_2 Using a Combination of Global Optimization and Data Mining, *Journal of Phase Equilibria and Diffusion*, 41 (2020) 538-549.
[24] J.P. Perdew, A. Zunger, Self-interaction correction to density-functional approximations for many-electron systems, *Physical Review B*, 23 (1981) 5048-5079.
[25] D. Zagorac, Zagorac, J., Doll, K, Čebela, M., Matović, B., Extreme pressure conditions of BaS based materials: Detailed study of structural changes, band gap engineering, elastic constants and mechanical properties, *Processing and Application of Ceramics* 13 (2019) 401-410.
[26] D. Jovanović, Zagorac, J., Matović, B., Zarubica, A., Zagorac, D., Structural, electronic and mechanical properties of superhard B4C from first principles, *Journal of Innovative Materials in Extreme Conditions*, 1 (2020) 12-18.
[27] J. Zagorac, Zagorac, D., Jovanović, D., Pejić, M., Škundrić, T., Matović, B., Ab initio investigations and behaviour of the α-Ce_2ON_2 phase in the extreme pressure conditions, *Journal of Innovative Materials in Extreme Conditions*, 2 (2021).
[28] J.C. Schoen, Energy Landscape Concepts for Chemical Systems under Extreme Conditions, *Journal of Innovative Materials in Extreme Conditions*, 2 (2021) 5-57.
[29] R. Hundt, KPLOT: A Program for Plotting and Analysing Crystal Structures, Technicum Scientific Publishing, Stuttgart, 2016.
[30] K. Momma, F. Izumi, VESTA: a three-dimensional visualization system for electronic and structural analysis, *Journal of Applied Crystallography*, 41 (2008) 653-658.
[31] S.K. Filatov, N.A. Bendeliani, B. Albert, J. Kopf, T.I. Dyuzheva, L.M. Lityagina, Crystalline structure of the TiO_2 II high-pressure phase at 293, 223, and 133 K according to single-crystal x-ray diffraction data, *Doklady Physics*, 52 (2007) 195-199.
[32] I.E. Grey, C. Li, I.C. Madsen, G. Braunshausen, TiO_2-II. Ambient pressure preparation and structure refinement, *Materials Research Bulletin*, 23 (1988) 743-753.
[33] M.E. Arroyo-de Dompablo, A. Morales-García, M. Taravillo, DFT+U calculations of crystal lattice, electronic structure, and phase stability under pressure of TiO2 polymorphs, *The Journal of Chemical Physics*, 135 (2011).
[34] P.Y. Simons, F. Dachille, The structure of TiO2II, a high-pressure phase of TiO_2, *Acta Crystallographica*, 23 (1967) 334-336.